Electronic Supplementary Material (ESI) for Biomaterials Science.

Supporting Information

Biomembrane induced in situ self-assembly of peptide with enhanced antimicrobial activity

Zhiwei Shen,[a,c] *Zhen Guo,*[a,c] *Limin, Zhou,*[a,b] *Yujiao Wang,*[a,c] *Jinjin Zhang,*[a,b] *Jun Hu,*[a,b] *Yi Zhang**[a,b]

[a]Key Laboratory of Interfacial Physics and Technology, Shanghai Institute of Applied Physics, Chinese Academy of Sciences, Shanghai 201800, China; [b]Zhangjiang Lab, Shanghai Advanced Research Institute, Chinese Academy of Sciences, Shanghai 201210, China; [c]University of Chinese Academy of Sciences, Beijing 100049, China

*Corresponding author. Email: zhangyi@sinap.ac.cn

Table S1. The secondary structures of AMPs analyzed with CDNN program.

195-260 nm	Helix	Antiparallel	Parallel	Beta -Turn	Random Coil
FF8 (pH=7.4)	10.36%	30.46%	11.49%	17.38%	30.31%
FF8 (pH=9.4)	8.75%	41.50%	9.92%	18.53%	21.23%
GG8 (pH=7.4)	9.45%	30.87%	11.74%	16.99%	30.95%
GG8 (pH=9.4)	8.23%	33.40%	11.77%	16.81%	29.86%

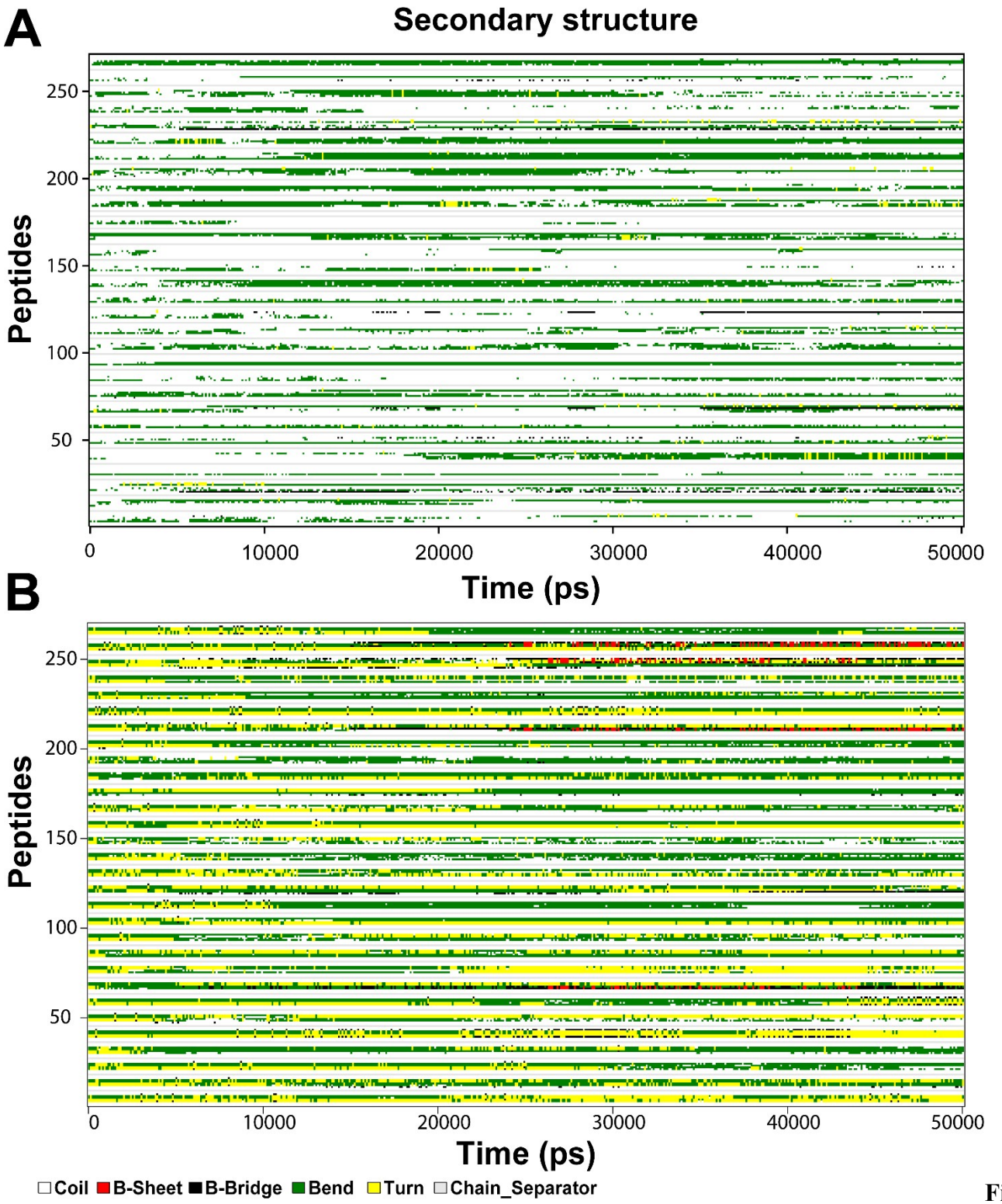

Fig. S1. DSSP plots for secondary structure transitions in deprotonted GG8 and FF8 during 50 ns MD simulations using the OPLSAA forcefields. (A) GG8 and (B) FF8. Results indicated that FF8 transformed to beta-sheet structures in aggregation process, while little changes in the secondary structures of GG8 were observed.

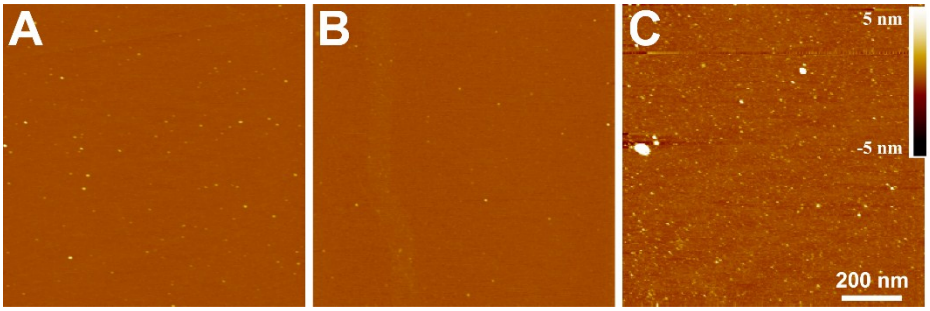

Fig. S2. AFM images indicating the effects of pH on the morphology of AMPs. (A) FF8 monomers (1mM) in PBS at pH 7.4; (B) GG8 monomers (1 mM) in PBS at pH 7.4; (C) GG8 monomers and aggregates in PBS at pH 9.4. The lateral and Z scale bars shown in (C) apply to all AFM images.

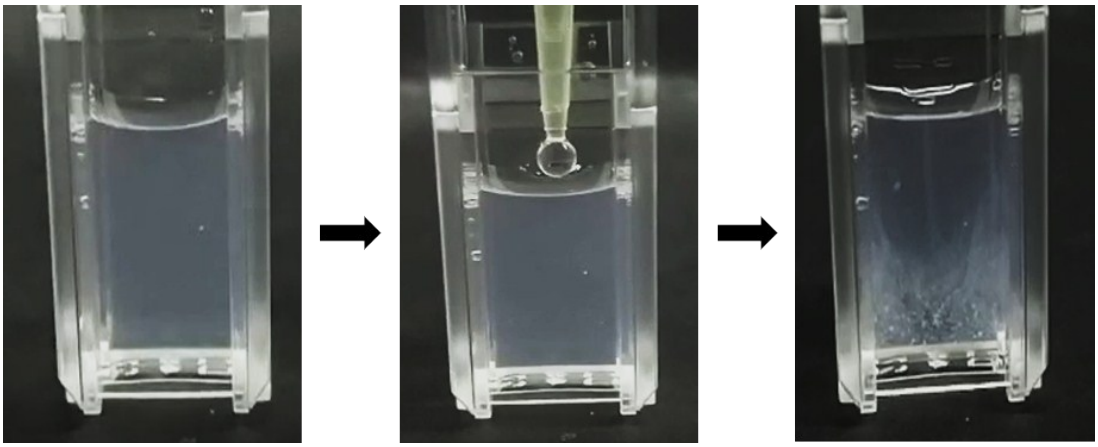

Fig. S3. Images indicating the aggtregation of AVs induced by cationic AMPs. Left and right panels: before and after adding FF8, respectively. Video indicating the aggtregation of AVs induced by cationic AMPs is also available.

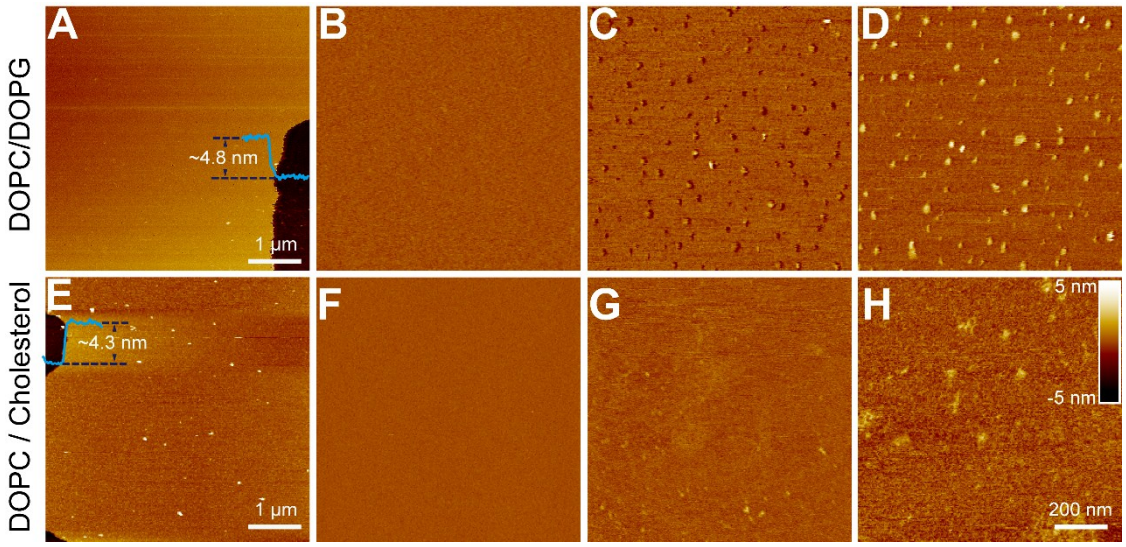

Fig. S4. AFM images of AMPs-treated lipid bilayers. (A-B) DOPC/DOPG bilayers on mica. Inset in A indicates a thickness of about ~4.8 nm for the bilayer as measured at its boundary. (C) DOPC/DOPG bilayer on mica after incubation with GG8 (200 µM) for 30 min at room temperature. (D) Image of the DOPC/DOPG bilayer in (C) after another 30 min at room temperature. (E-F) DOPC/Cholesterol bilayers on mica. Inset in E indicates a thickness of about ~4.3 nm for the bilayer as measured at its boundary. (G) DOPC/Cholesterol bilayer on mica after incubation with GG8 (200 µM) for 30 min at room temperature. (H) DOPC/Cholesterol bilayer after incubation with FF8 (200 µM) for 30 min at room temperature. The lateral scale bar shown in (H) applies to (B-D) and (F-H). The Z scale bar in H applies to all AFM image.

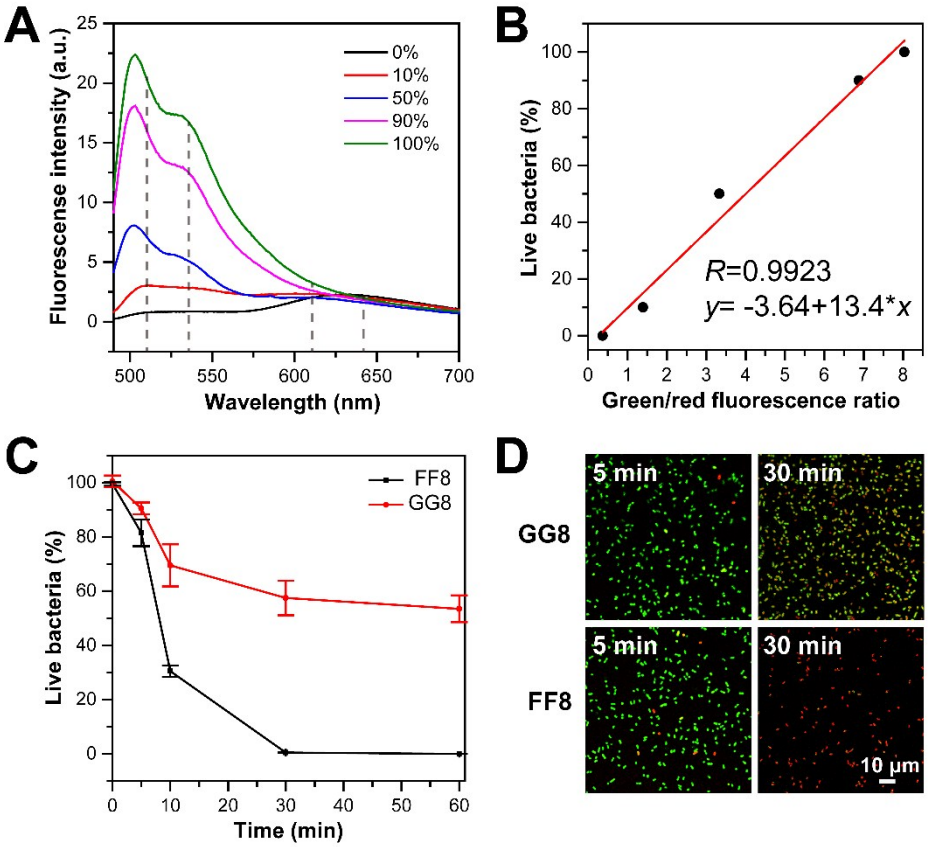

Fig. S5. Bactericidal effects of AMPs against *E. coli.* (A) Fluorescence spectra of suspensions of live and isopropyl alcohol–killed *E. coli* with various proportions. (B) The plot of the proportion of live bacteria in the suspension against the Green/red fluorescence ratio. The green fluorescence represents that bacteria is live while red fluorescence represents dead. The intensities of the green fluorescence in the range of 510-540 nm and the red fluorescence in the range of 610-640 nm were employed for calculating of each proportion of live/dead *E. coli*. (C) Bactericidal curves of 50 μM GG8 and FF8 against *E. coli*. Live bacteria was quantified with the curve in (B). N=3. (D) Representative fluorescence images of *E. coli* after treatment with GG8 or FF8 for 5 min and 30 min, respectively.

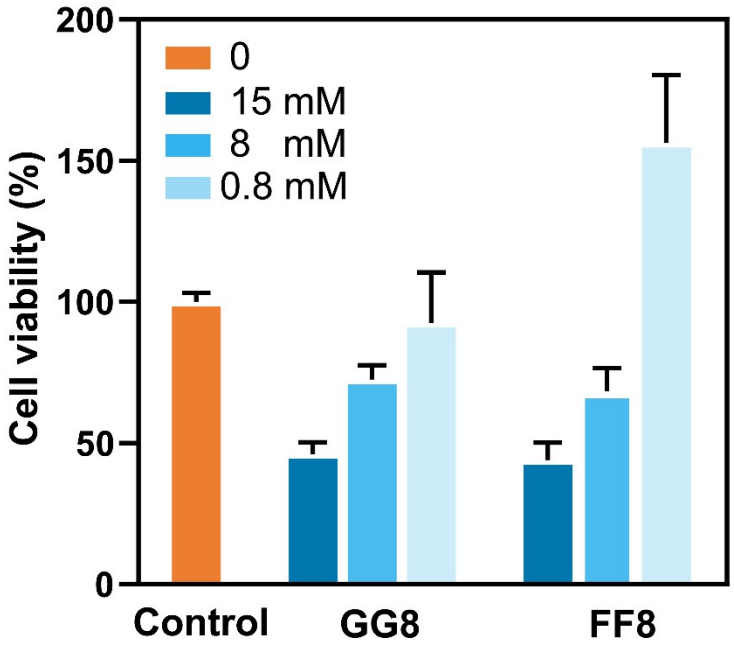

Fig. S6. Effect of AMPs on cell viability. Hela cells were treated with GG8 or FF8 at different concentrations (15 mM, 8 mM, or 0.8 mM). In the control group, the Hela cells were treated with PBS. Data were expressed as the mean ± SD (standard deviation) from at least three independent experiments.